

The mechanochemical Scholl reaction – a solvent-free and versatile graphitization tool

Sven Grätz^a, Doreen Beyer^b, Valeriya Tkachova^b, Sarah Hellmann^a, Reinhard Berger^b, Xinliang Feng^b and Lars Borchardt^{*a}

a Professur für Anorganische Chemie I, Technische Universität Dresden, Bergstraße 66, D-01069 Dresden, Germany.

b Professur für molekulare Funktionsmaterialien, Technische Universität Dresden, Mommsenstr. 4, D-01069 Dresden, Germany.

Table of Contents

1	General methods.....	2
2	Materials	2
3	Synthetic Procedures	3
	3.1 Synthesis of Precursors	3
	3.2 General Mechanochemical Cyclodehydrogenation procedure.....	5
	3.3 Mixer mill.....	8
4	Characterization	9
5	Optimization - Design of Experiment	16
6	¹ H-NMR spectra of the precursors	18
7	References.....	21
8	Author contributions.....	21

1 General methods

Ball mill syntheses were carried out in a Fritsch Pulverisette 7 premium line planetary ball mill operating at a rotation speed of 800 rpm. The syntheses were performed in a 45 mL zircon dioxide grinding jar with 22 zircon dioxide balls (10 mm in diameter) if not stated otherwise. Additionally a Retsch MM400 with a 20 ml tempered steel milling jar and 4 tempered steel balls (10 mm in diameter) at 25 Hz and 30 minutes was used. For the synthesis in the MM no bulking material was used.

Bulking material: Briefly, a bulking agent can be interpreted as an inert additive to the reaction. The size of the milling jar (45 mL in our case) requires a minimum amount of reactants in the reaction jar (ball-to-powder ratio), otherwise the milling balls will collide without transferring the energy of the collision onto the reactants, thus causing enhanced abrasion. We used an inert bulking agent - NaCl - to gain control over the reactions scale. This method was first described by Konnert et Al.¹ Since we used a total mass loading of 10 g in the milling jar for all runs, we added the amount of bulking agent that was necessary to reach 10 g. Alternatively we could have also increased the amount of FeCl₃ to deal with this issue.

Matrix assisted laser desorption ionization time of flight mass spectroscopy (MALDI-TOF) was carried out on a Bruker Autoflex Speed spectrometer using a 337 nm nitrogen laser with Tetracyanoquinodimethane as matrix if not indicated otherwise.

Proton Nuclear magnet resonance spectroscopy (¹H-NMR) was recorded in deuterated Dichloromethane (CD₂Cl₂) solution at room temperature, using a BRUKER AC 300 P instrument.

Scanning electron microscopy (SEM) images were obtained using a Hitachi SU8020 SEM equipped with a secondary electron (SE) detector. Prior to the measurement the samples were prepared on an adhesive carbon pad and sputtered with gold to obtain the necessary electron conductivity.

Solid state UV/Vis (ss-UV/Vis) measurements were conducted on a VARIAN Cary 4000 with a HARRICK Praying Mantis unit. The step width was set to 1 nm and the sources were switched at 350 nm. The crude samples were mixed with an excess of BaSO₄ prior to measuring.

UV/Vis spectra were measured on UV-Vis-NIR Spectrophotometer Cary 5000 at room temperature using a 10 mm quartz cell.

2 Materials

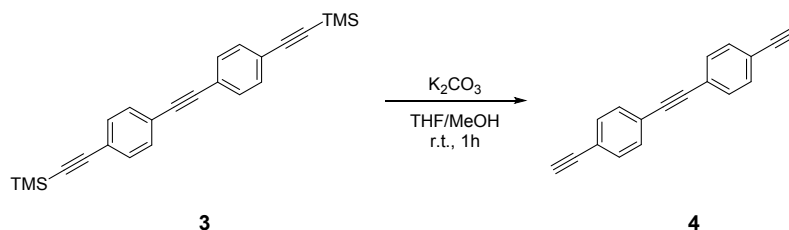
Hexaphenylbenzene (TCI), Iron(III) chloride (anhydrous; ABCR, >98%), Molybdenum(V) chloride (anhydrous; ABCR, 99.6%) and Sodium chloride (Güssig, >98%) were used as received. 2-Bromoacetophenone (TCI), Trifluoromethanesulfonic acid (Sigma Aldrich, 98%), 4-Biphenylboronic acid (Activate Scientific, 98%), Tetrakis(triphenylphosphine)palladium(0) (Strem Chemicals, 99%), Bis(4-bromophenyl acetylene) (Fisher Scientific, 97%), Copper(I) iodide (Strem Chemicals, 98%), Ethynyltrimethylsilane (Sigma Aldrich, 98%), Dichloro(triphenylphosphine)palladium(II) (Strem Chemicals, 99.9%), Tetraphenylcyclopentadienone (Fisher Scientific, 99%) and Cobalt carbonyl (Strem Chemicals, 95%) and Triphenylphosphine (Sigma Aldrich, 99%) were used as received without further purification.

Zirconium oxide (Type ZY-S) milling balls with a diameter of 10 mm were purchased from Sigmund Lindner GmbH. The average weight of one milling ball is 3.19 ± 0.05 g.

Tempered steel (1.4125, AISI 440C) milling balls with a diameter of 10 mm were purchased from TIS Wälzkörpertechnologie GmbH. The average weight of one milling ball is 4.02 ± 0.02 g.

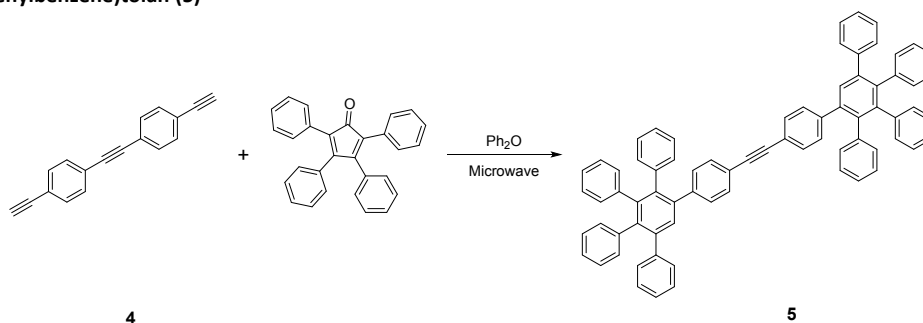
acetate, washed with brine and dried over Magnesiumsulfate. The crude product was further cleaned by silica gel chromatography with Ethyl acetate/*iso*-Hexane 1:9 as eluent. Title compound **3** was obtained as light grey solid (4g, yield: 81 %). ¹H-NMR (CD₂Cl₂, 300 MHz): 7.49 – 7.42 (m, 8H), 0.26 (s, 18H). The spectroscopic data of compound **3** are consistent with those described in literature.⁴

4,4'-Diethynyltolan (**4**)



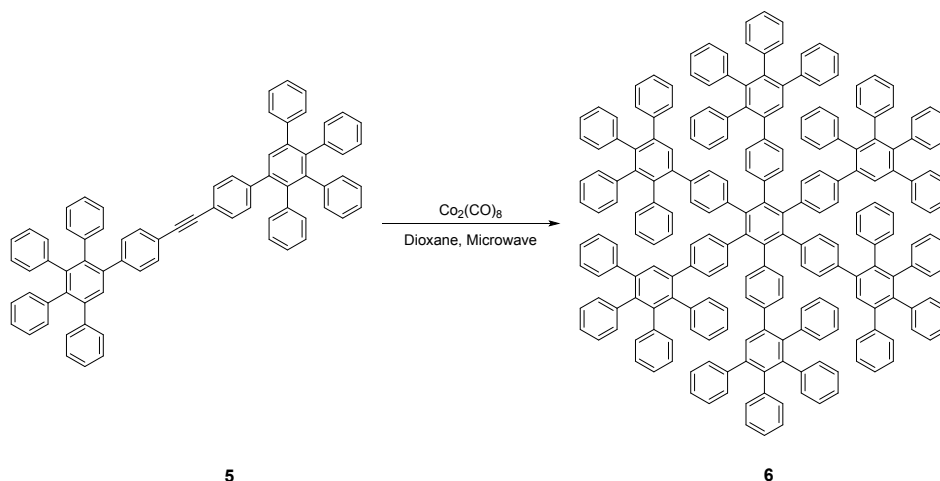
In a round bottom flask, containing a 1:1 mixture of Methanol and Tetrahydrofuran (30 ml : 30 ml), was charged with 1.72 g (5.7 mmol, 2.2 eq.) Potassium carbonat and intensively degassed with argon. Compound **3** (2.1 g, 5.7 mmol, 1 eq.) was added in one portion and the solution was maintained at room temperature for 1 h until completion. The reaction mixture was quenched with deionized water, extracted with Ethyl acetate, washed with brine and dried over Magnesiumsulfate. After standard work-up procedure the resulting crude target compound **4** (720 mg, yield: 56 %) was directly used without further purification for the next step. ¹H-NMR (CD₂Cl₂, 300 MHz): δ 7.46 (d, *J* = 19.2 Hz, 8H), 3.26 (s, 2H) ppm. The spectroscopic data of compound **4** are consistent with those described in literature.⁴

4,4'-(2,3,4,5-Tetraphenylbenzene)tolan (**5**)



300 mg (1.3 mmol, 1 eq.) of compound **4** and 1.13 g (2.9 mmol, 2.2 eq.) Tetraphenylcyclopentadienone were dissolved in 5 ml Diphenylether. The microwave-assisted Diels-Alder reaction was performed under inert conditions with the mono-mode microwave reactor "Discover SP-D" from CEM. Implemented microwave conditions: 250 °C, 300 W, power max: *on*, stirring speed: *medium*, 12 h. The obtained reaction mixture was precipitate in 200 ml *iso*-Hexane. The light brown precipitate was filtered and washed with Methanol to afford compound **5** as brownish solid (650 mg, 52 %). ¹H-NMR (CD₂Cl₂, 300 MHz): δ 7.52 (s, 2H), 7.35 – 6.79 (m, 48H) ppm. The spectroscopic data of compound **4** are consistent with those described in literature.⁴

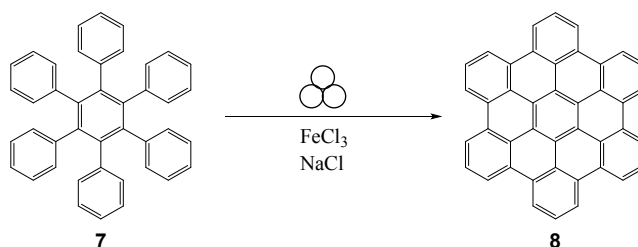
1,2,3,4,5,6-Hexakis(4',5',6'-triphenyl-1,1':2',1''-terphenyl)benzene (6)



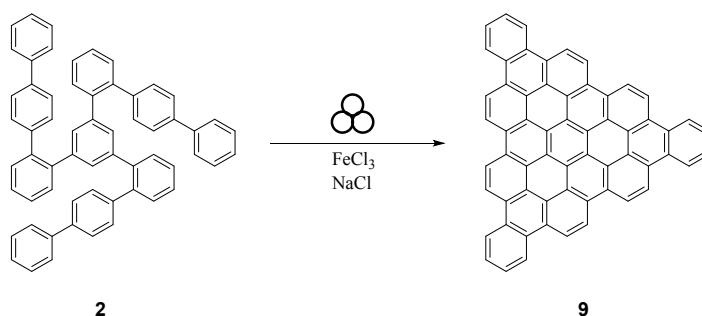
100 mg (106 μmol , 1 eq.) of compound **5** and 8.5 mg (25 μmol , 0.7 eq.) Cobalt carbonyl were dissolved in 1.5 ml Dioxane and intensively degassed with argon. The microwave-assisted cyclotrimerization reaction was performed at 160 $^{\circ}\text{C}$, 300 W, power max: *on*, stirring speed: *medium*, 4 h. The reaction mixture was precipitate in 10 ml *iso*-hexane. Afterwards the crude solid was purified by silica gel column, using Ethyl acetate/*iso*-Hexane 1:4 as eluent. Title compound **6** was obtained as off-white solid (350 mg, yield: 44 %). $^1\text{H-NMR}$ (CD_2Cl_2 , 300 MHz): δ 7.40 (s, 6H), 7.14 (s, 30H), 7.01 – 6.70 (m, 90H), 6.63 (d, $J = 8.3$ Hz, 12H), 6.37 (d, $J = 8.3$ Hz, 12H) ppm. The spectroscopic data of compound **4** are consistent with those described in literature.⁴ MALDI-TOF (DCTB): 2820.69, calc. 2817.18.

3.2 General Mechanochemical Cyclodehydrogenation procedure

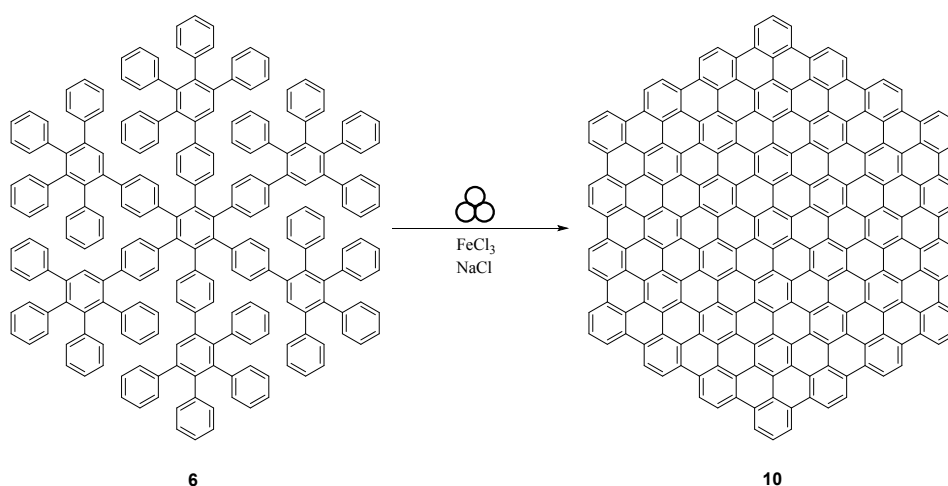
Hexabenzocoronene (8)



In a typical synthesis, 0.1 g HPB **7** (0.187 mmol), 2.184 g iron chloride (13.5 mmol, 72 eq.) and the inert bulking material 7.716g sodium chloride were transferred into a 45 mL zirconium oxide grinding jar with twenty-two zirconium oxide 10 mm-diameter grinding balls (3.19 g each). The educts were then milled for 60 min at 800 rpm in a Fritsch Pulverisette 7 premium line planetary ball mill. After the reaction, the grinding jar was opened and the reaction mixture was poured into water. The crude product was consequently washed with water, methanol and ethanol before it was dried at 80 $^{\circ}\text{C}$. HBC **8** was obtained as a red solid (93 mg, yield: 95%). MALDI-TOF (**SFig. 10**) (TCNQ): 522.40, calc. 522.14.

C60 (9)

For C60 the protocol was changed in the following manner: 0.1 g of 1,3,5-tris(2-1,1':4',1''-Terphenyl)benzene **2** (0.131 mmol), 2.295 g iron chloride (14.1 mmol) and the inert bulking material 7.605 g sodium chloride were transferred into a 45 mL grinding jar with twenty-two 10 mm-diameter grinding balls. The educts were then milled for 60 min at 800 rpm in a Fritsch Pulverisette 7 premium line planetary ball mill. After the reaction, the grinding jar was opened and the reaction mixture was poured into water. The crude product was consequently washed with water, methanol and ethanol before it was dried at 80°C. C60 **9** was obtained as a red solid (79 mg, yield: 81%). MALDI-TOF (**SFig. 11**) (TCNQ): 743.95, calc. 744.19.

C222 (10)

For C222 the protocol was changed in the following manner: 0.05 g of 1,2,3,4,5,6-Hexakis(4',5',6'-triphenyl-1,1':2',1''-terphenyl)benzene **6** (0.018 mmol), 1.865 g iron chloride (11.5 mmol) and the inert bulking material 8.085 g sodium chloride were transferred into a 45 mL grinding jar with twenty-two 10 mm-diameter grinding balls. The educts were then milled for 60 min at 800 rpm in a Fritsch Pulverisette 7 premium line planetary ball mill. After the reaction, the grinding jar was opened and the reaction mixture was poured into water. The crude product was consequently washed with water, methanol and ethanol before it was dried at 80°C. C222 **10** was obtained as a black solid (43mg, yield: 89%). MALDI-TOF (**SFig. 11**) (TCNQ): 2711.02, calc. 2708.34.

Table S1. Investigation of the milling material

sample	milling material	yield ^[a]	comment
HBC-1	zirconium dioxide	95	-
HBC-2	tempered steel	.. ^[b]	excessive abrasion
HBC-3	tungsten carbide	.. ^[b]	excessive abrasion
HBC-4	silicone nitride	97	-

All experiments were conducted with HPB, at 800 rpm, with 22x 10 mm balls, a milling time of 60 min and 12 eq. of FeCl₃ per H

^[a] yield after purification

^[b] abrasion of the milling material in combination of excessive chlorination lead to abrasion of the milling material in combination of excessive chlorination makes the determination of a yield of HBC impossible

Table S2. Investigation of the milling time (HPB-t) and speed (HPB-s)

sample	rpm [min ⁻¹]	milling time [min]	yield ^[a]
HBC-t-30	800	30	95
HBC-t-60	800	60	95
HBC-t-90	800	90	.. ^[b]
HBC-t-120	800	120	88
HBC-s-100	100	60	12 ^[c]
HBC-s-200	200	60	95 ^[c]
HBC-s-400	400	60	94 ^[c]
HBC-s-600	600	60	99 ^[c]
HBC-s-800	800	60	95 ^[c]

All experiments were conducted, with HPB, 22x 10 mm zirconium dioxide balls, and 12 eq. of FeCl₃ per H

^[a] yield after purification

^[b] MALDI-TOF TOF measured from a small sample of the 2h synthesis taken after 1 h

^[c] Conducted in a GTM vessel for in-situ investigation

Table S3. Scope of the starting materials, capture of HCl (HPB-lp) and transfer to the mixer ball mill (HPB-mm)

sample	starting material	milling material	rpm [min ⁻¹]	milling time [min]	yield ^[a]
C60	C60H42 (2)	zirconium dioxide	800	60	81 ^[b]
C222	C222H150 (6)	zirconium dioxide	800	60	89 ^[b]
HBC-lp-1	HPB + Pyridine	zirconium dioxide	800	30	91 ^[b]
HBC-lp-2	HPB + Ethanol	zirconium dioxide	800	30	45 ^[b]
HBC-lp-2	HPB + Ethanol	zirconium dioxide	800	60	97 ^[b]
HBC-mm	HPB	tempered steel	25 Hz	30	58 ^[c]

All experiments were conducted, 22x 10 mm zirconium dioxide balls, and 12 eq. of FeCl₃ per H if not state otherwise

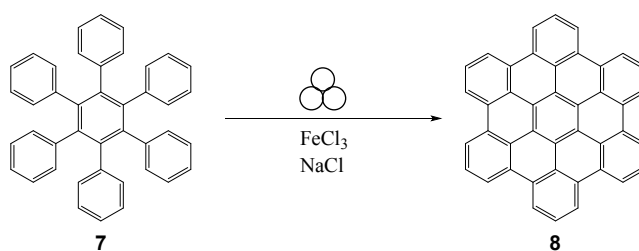
^[a] yield after purification

^[b] Conducted in a GTM vessel for in-situ investigation

^[c] Mixer ball mill: 0.1 g HBP, 2.184 g FeCl₃, 4x 10 mm balls

3.3 Mixer mill

Additionally we conducted a proof-of-principal experiment in a mixer-mill. Since those mills are generally equipped with smaller milling jars one can hereby apply our approach to a few mg-scale suitable for the development of unprecedented, more complex PAHs. Furthermore, the in-situ techniques reported are all conducted in mills based on this principle.⁵⁻¹⁰ However, the transfer of protocols between two mill types bears many challenges and a separate optimization of reaction parameters has to be conducted for mixer mills. The yield after 30 minutes is lower than in the planetary equivalent but an increase in either reaction time, or vibration frequency, as well as an adjustment of milling balls (size and number) should produce comparable results in the future.



In the mixer mill synthesis, 0.1 g HPB **7** (0.187 mmol), 2.184 g iron chloride (13.5 mmol, 72 eq.) chloride were transferred into a 20 mL tempered steel grinding jar with four 10 mm-diameter steel grinding balls (4.02 g each). The educts were then milled for 30 min at 25 Hz in Retsch MM400 mixer mill. After the reaction, the grinding jar was opened and the reaction mixture was poured into water. The crude product was consequently washed with water, methanol and ethanol before it was dried at 80°C. HBC **8** was obtained as a red solid (57 mg, yield: 58%).

4 Characterization

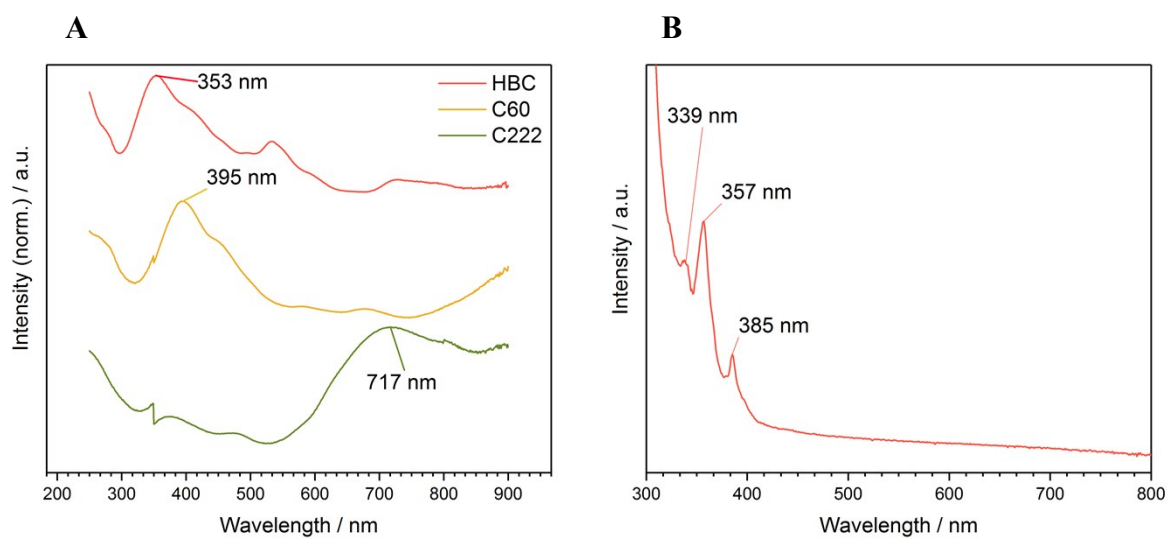


Fig. S1. A: ss-UV/Vis measurement of HBC (red), C60 (yellow) and C222 (green) with the respective maxima given in the graph. As expected with an increasing size of the π -network, we can observe a bathochromic shift of the adsorption maxima from 353 nm HBC to 395 nm in C60 and 717 nm in C222. B: UV/Vis measurement of HBC in toluene ($c = 1.1 \cdot 10^{-5} \text{ mol l}^{-1}$) showing the peaks reported in the literature.

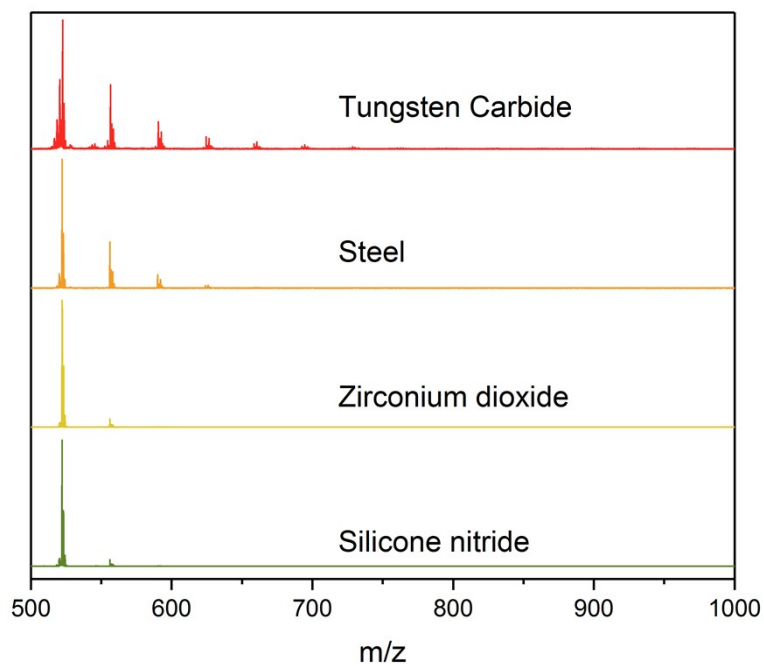


Fig. S2. MADLI-TOF measurements of the HBC system milled with different milling material. Conditions: 800rpm, 22 balls, 60 min. A clear trend towards higher chlorination with higher density milling materials and therefore high impact energies can be observed. Experimental details are given in Table S1.

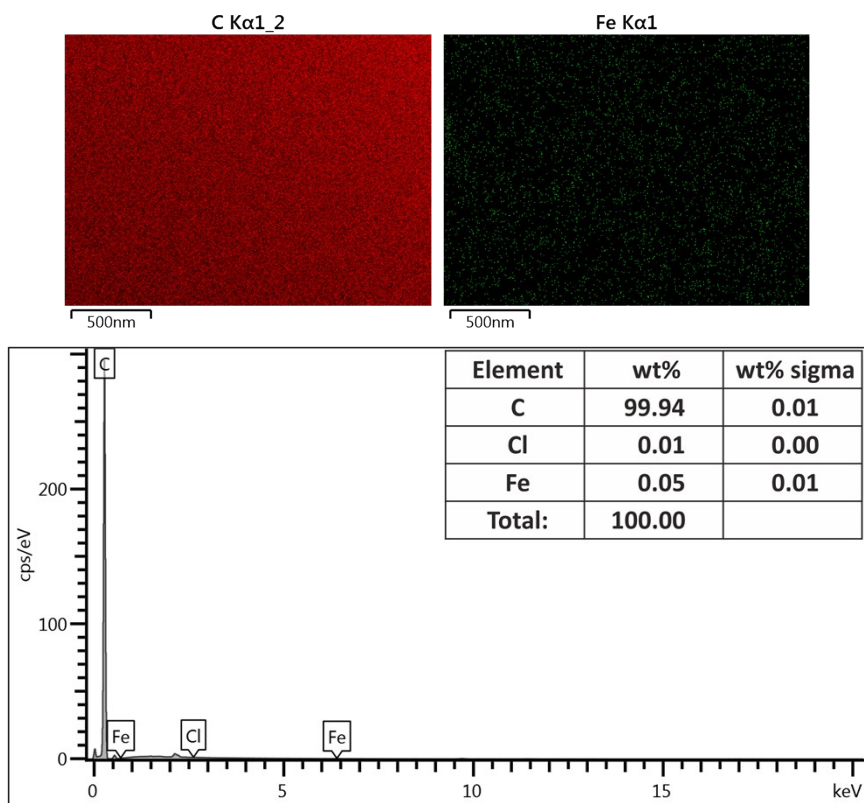
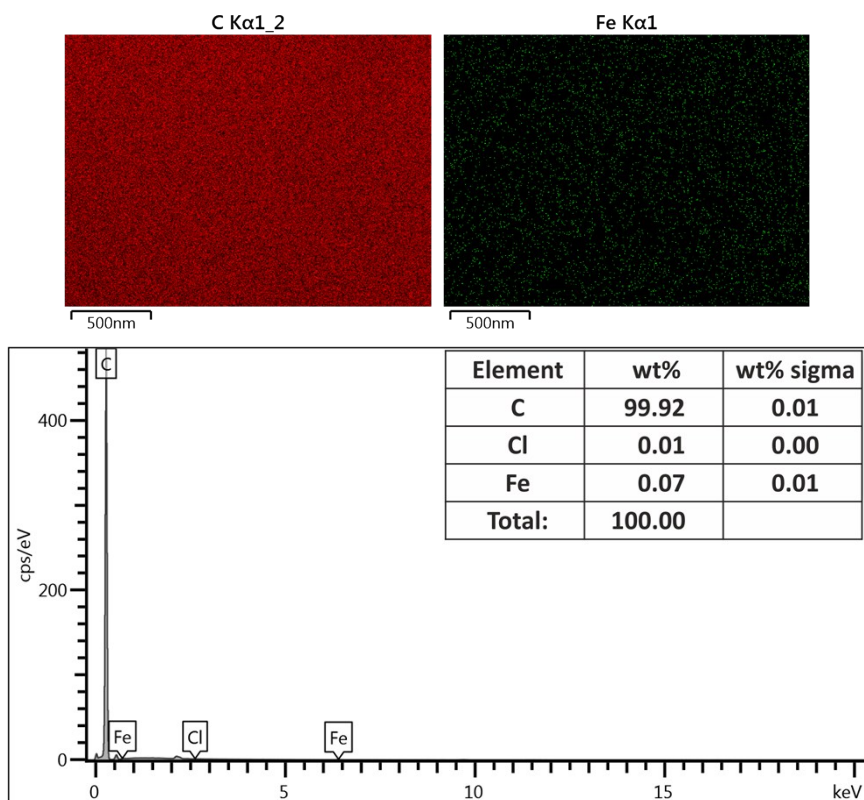
A**B**

Fig. S3. EDX mapping at two different spots of the sample milled for 30 minutes at 800 rpm with 22 zirconium dioxide balls. (A and B) revealing a neglectable amount of iron in the sample. The mapping data is calculating 0.05 wt% (A) and 0.07 wt% (B) of iron respectively which is below the limit of detection for this method. No zirconium was detected at all. This confirms the purity of our samples. Gold used for sputtering was excluded from the quantification.

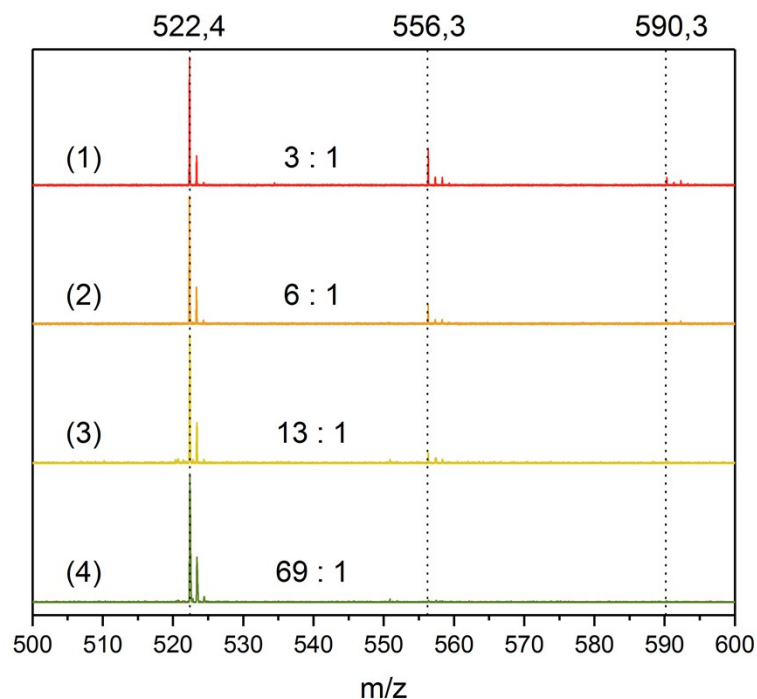


Fig. S4. MADLI-TOF measurements of the HBC system milled for different reaction times. Conditions: 800rpm, 22 balls, 30min (4), 60 min (3), 90 min (2) and 120 min (1). The ratio between HBC (522.4) and the monochloro adduct (556.3) are given. A clear trend towards higher chlorination with longer milling time can be observed. Experimental details are given in Table S2.

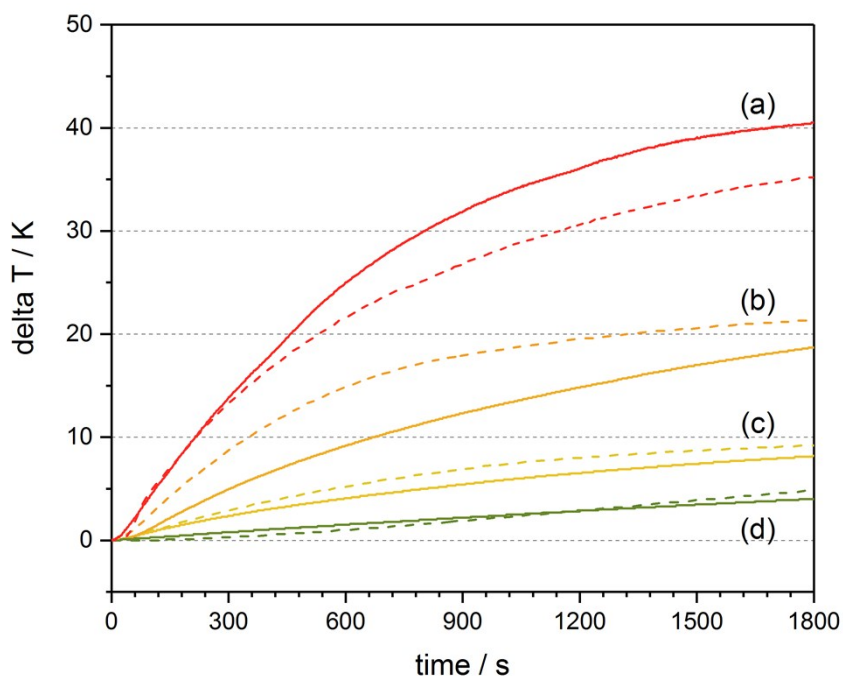


Fig. S5. Development of the relative vessel temperature during the milling process of HPB (bold lines) and the reference without HPB (dashed lines) for different milling speeds. (a) 800 rpm, (b) 600 rpm, (c) 400 rpm and (d) 200 rpm. The temperature differences between the reference sample and the reaction with HPB is not very sensitive because of the small amount of reactants in the vessel. Therefore external factors like vessel temperature at the start of the milling process have a big impact on the measurement. Therefore we decided to not use the vessel temperature as an indicator of reaction progress

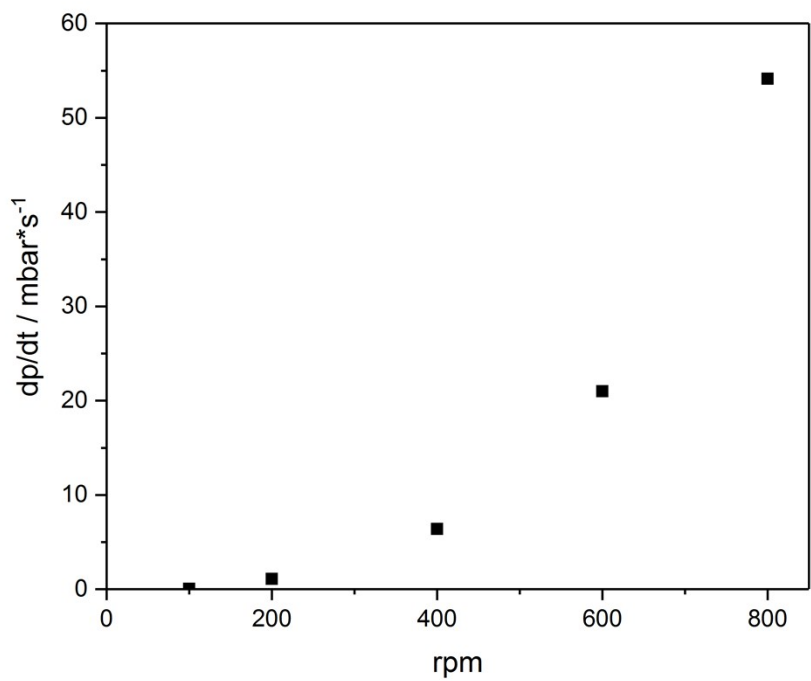


Fig. S6. Changes in the slope of the pressure rise vs the rpm of the milling vessel. Since the energy input increases with the square of the milling speed this curve from has to be expected. At 100 rpm no reaction could be observed.

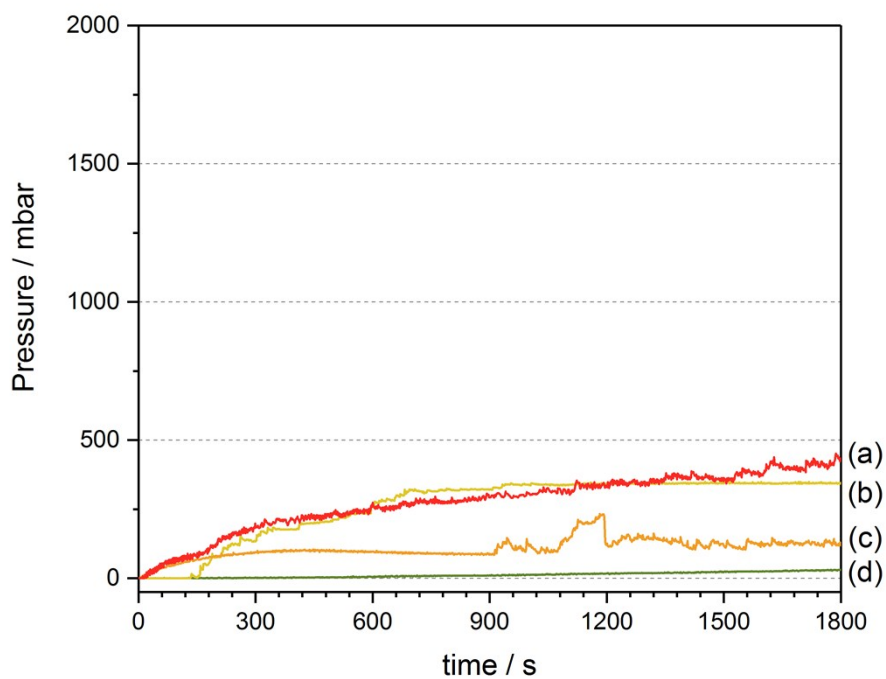


Fig. S7. Development of the relative vessel pressure during the milling process without HPB for different milling speeds. (a) 800 rpm, (b) 600 rpm, (c) 400 rpm and (d) 200 rpm. The pressure in these reference experiments only rises due to the heating of the milling vessel. This heating is dependent of the milling speed – at lower rpm the dissipated heat is smaller. Therefore samples milled at low speeds experience only a small pressure rise.

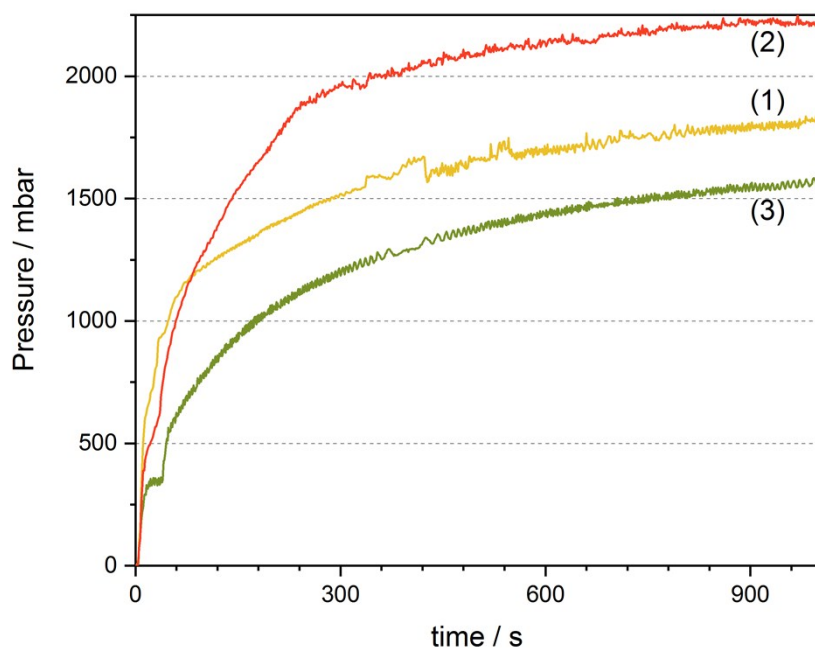


Fig. S8. Development of the relative vessel pressure during the milling process A: comparison of HCB (1) with C60 (2) at 400 rpm. A: comparison of HCB (3) with C222 (4) at 800 rpm. For all samples a swift rise in pressure can be observed. After this first steep increase (~300s) it transitions into a smaller sloped ascend due to the rise in vessel temperature.

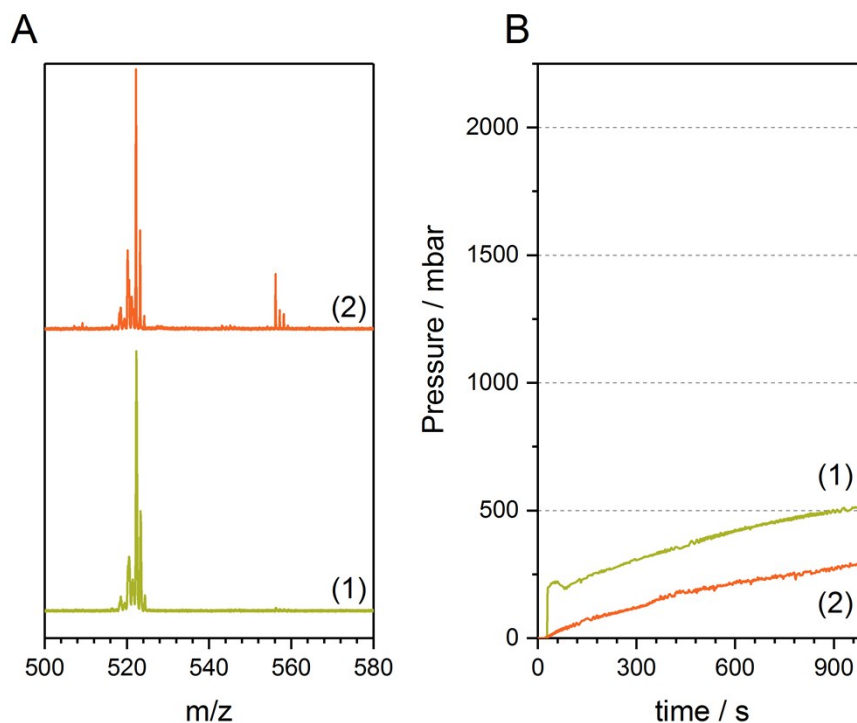


Fig. S9. A: MADLI-TOF measurements of the HBC system milled with the addition of pyridine (HBC-lp-1; (1)) and ethanol (HBC-lp-2; (2)). For (1) only the target mass of 522 m/z can be observed while for (2) small amounts of the monochloro adduct are also visible. B: Development of the relative vessel pressure during the milling process of HBC-lp-1 (1) and HBC-lp-2 (2) at 800 rpm. The pressure rise in both cases is very low (in the range of the pressure rise of the reference sample) compared to the samples run without any additives.

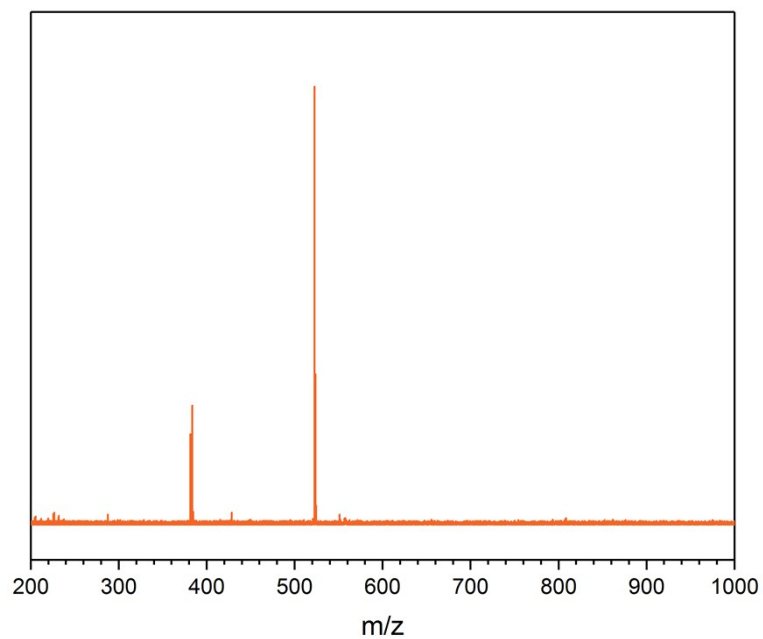


Fig. S10. Complete MADLI-TOF measurements of the HBC system milled at 800 rpm.

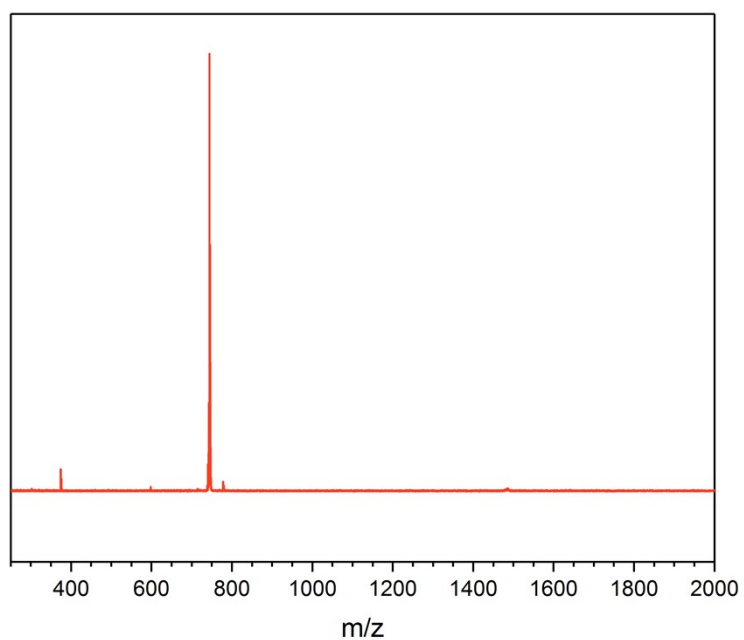


Fig. S11. Complete MADLI-TOF measurements of the C60 system milled at 800 rpm.

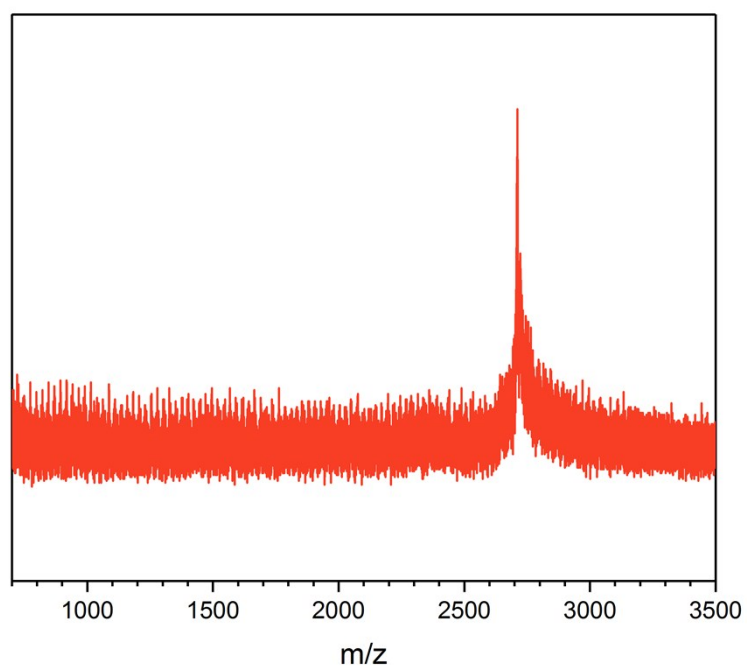


Fig. S12. Complete MADLI-TOF measurements of the C222 system milled at 800 rpm.

5 Optimization - Design of Experiment

Design of experiments describes a methodological variation of parameters in order to get the most information out of a minimum number of experiments. The data is therefore collected and a regression function is calculated in order to fit the investigated result (e.g. yield) with the chosen parameters in order to determine their influence. Since it is a statistical approach the variance of the experiment is taken into consideration as well. This can be accomplished by repeating certain experiments. It is beneficial to repeat the centre points that are introduced into the set-up to detect non-linear behaviour because their all parameters are at under non-extreme conditions. The choice of parameters and their step size is crucial for precise results. It should be noted that it is in general better to choose them in such a manner as to obtain maximum effects, to better differentiate the effects from the normal variance. Furthermore the runs are conducted in a randomized order to spread influence from random disturbances (different batches of starting material, lab temperature, etc.) evenly over all experiments.

The impact of the synthesis parameters applied on the mechanochemical Scholl reaction were studied in a factorial 2^{7-3} factorial design with a resolution of IV with a centre point that was repeated once. The parameters are varied in 2 levels, as represented in Table S4.

Table S4. 2 level, fractional DOE layout with center points, randomized order.

run order	rpm	ball size	ball/powder ratio	milling time	eq. FeCl ₃	yield
1	200	15	45	30	12	45
2	800	10	45	30	12	80
3	800	15	9	10	72	64
4	200	10	9	30	12	89
5	500	10	27	20	42	70
6	200	15	45	10	72	70
7	200	15	9	30	72	15
8	500	10	27	20	42	67
9	800	15	9	30	12	63
10	200	10	45	10	12	63
11	800	10	45	10	72	80
12	800	10	9	10	12	12
13	800	15	45	10	12	31
14	200	15	9	10	12	42
15	200	10	9	10	72	48
16	200	10	45	30	72	76
17	800	10	9	30	72	63
18	800	15	45	30	72	92
19	500	15	27	20	42	59
20	500	15	27	20	42	67

The main and interaction effect plots for the yield of the reaction are given in Figure S10. The main effect plots can give one an idea of the influence of a single parameter. For the rpm of the ball mill the influence on the reaction is rather small. The yield at 200 and 800 rpm are varying in around 5%. The red centre point is at a medium speed but the influence of other parameters is also taken into accounts so it cannot be understood as an influence of the milling speed. For the ball size the picture is different. Here we can see a big influence on the yield. An increase in ball size is leading to a smaller yield. This is likely due to differences in the milling dynamic with bigger balls were the impact energy is higher but the number of impacts overall is lower. In addition in order to obtain a fine powder the balls have to be a small as possible, so bigger balls can lead to a decreased surface of the powder during the reaction. The third graph describes the influence of the ball to powder ratio. This parameter has big implications to the milling process. It is the weight ratio of the balls (22 balls weight 90 g) to the total powder in the ball mill. If there is less powder the trajectory of the milling balls is influenced and more energy is transferred to the powder. If too much powder is utilized the ball movement is hindered and the transfer of energy is decreased. In our study a lower amount of powder and therefore higher energies seem to favour the reaction. The milling time and equivalents of FeCl₃ have an obvious effect on the reaction showing an increase in yield with an increase of either one of these parameters. The centre point mention earlier seems to be heavily influenced by the last three discussed parameters which indicates a non-linear behaviour.

In the interaction plot the interactions of the different parameters are visualized. If two parameters are independent the graphs are parallel. If they are interacting however, the curves are crossing each other. The strongest interaction can be observed between the reaction time and the eq. of iron chloride. As it was expected a bigger amount of reagent is leading to a shorter necessary reaction time. Similarly the interaction between the rpm and the eq. of FeCl₃ is showing that at lower speeds an increase of reagent is leading to higher yields.

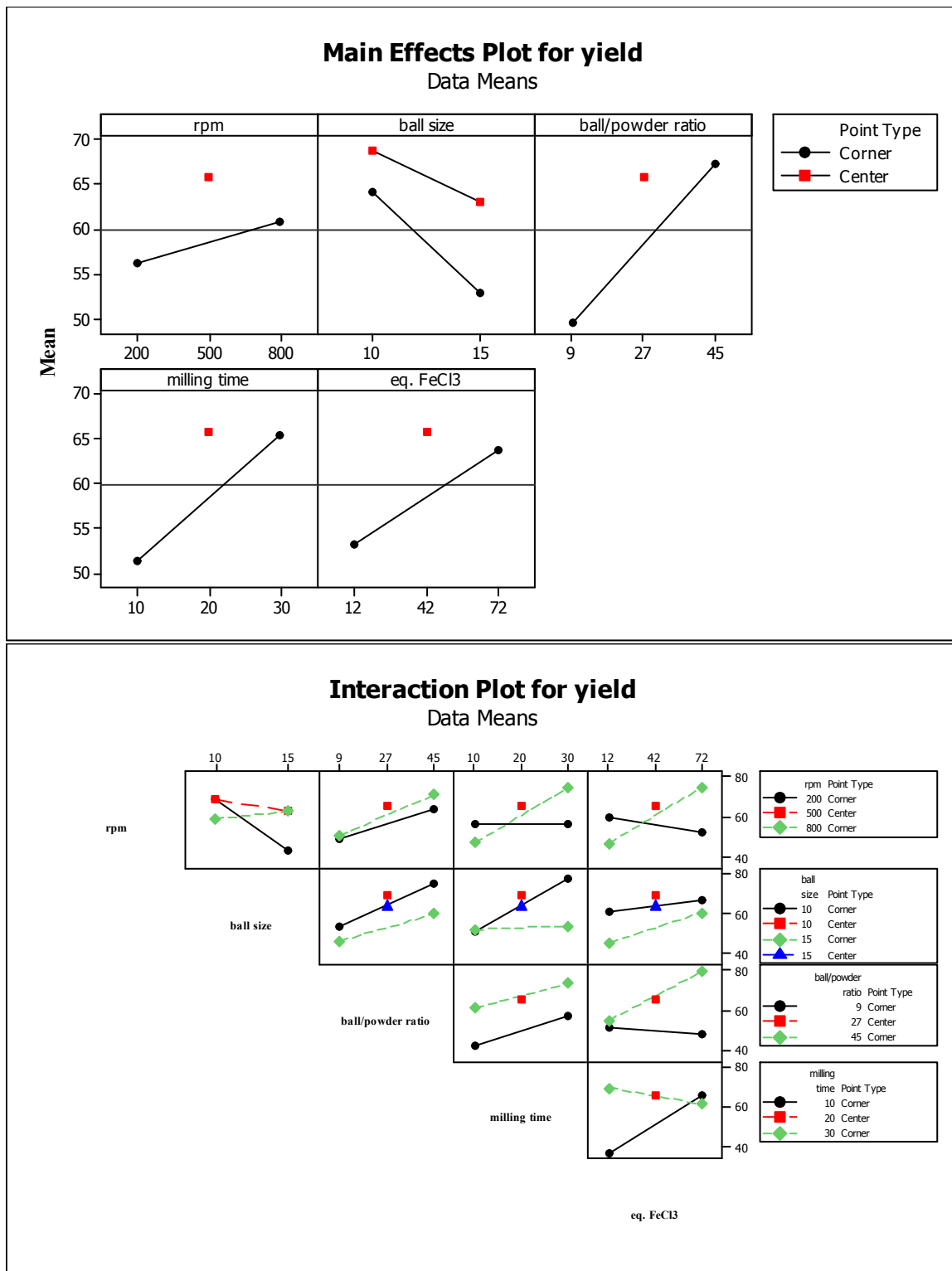


Fig. S13. Results of the DOE (cf. TableS4). The main and interaction plots of the parameters: rpm, ball size, ball/powder ratio, milling time and eq. FeCl₃ are presented.

6 $^1\text{H-NMR}$ spectra of the precursors

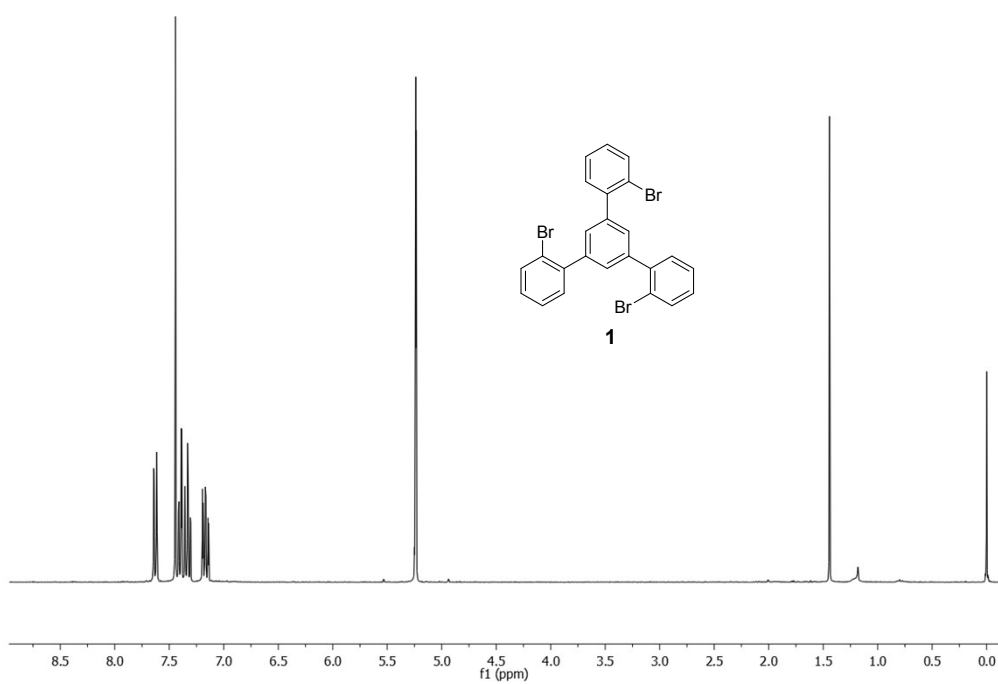
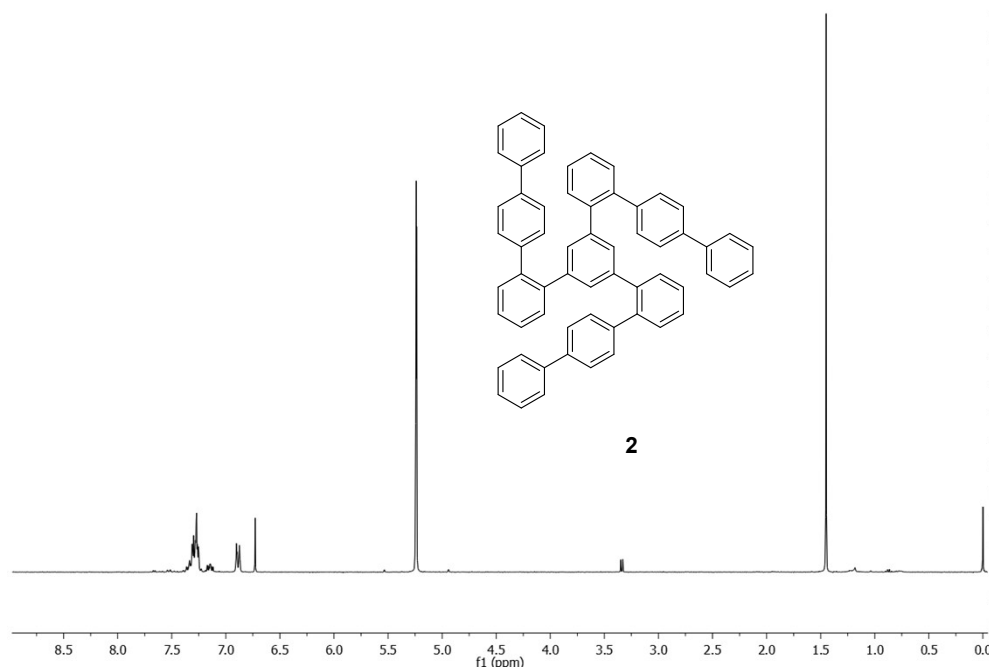


Fig. S14 $^1\text{H-NMR}$ spectra of 1,3,5-tris(2-bromophenyl)benzene (**1**) in CD_2Cl_2



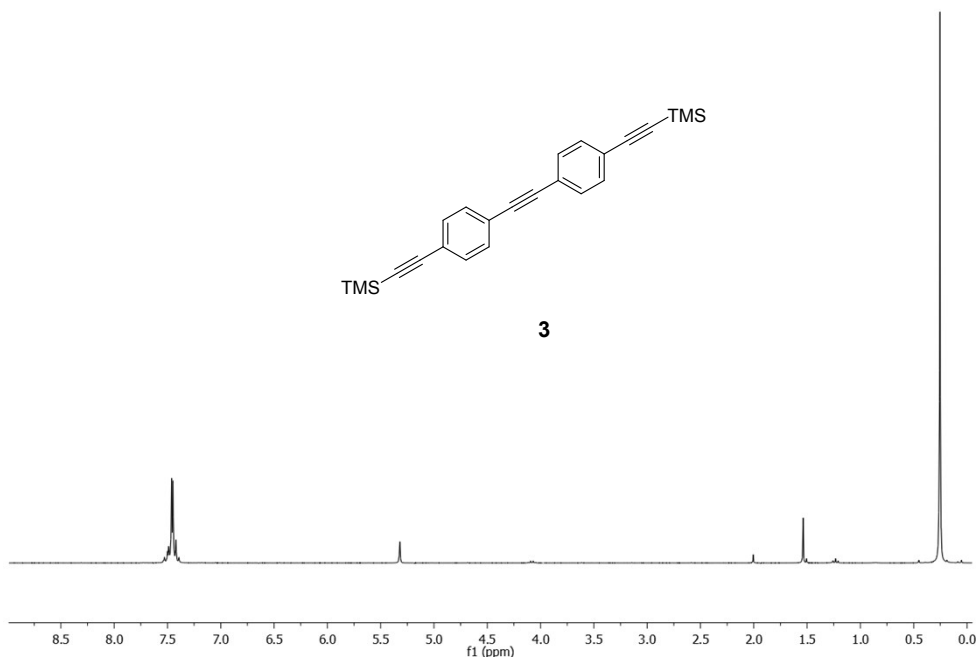


Fig. S16 ¹H-NMR spectra of 4,4'-Bis[(trimethylsilyl)ethynyl]tolane (3) in CD₂Cl₂

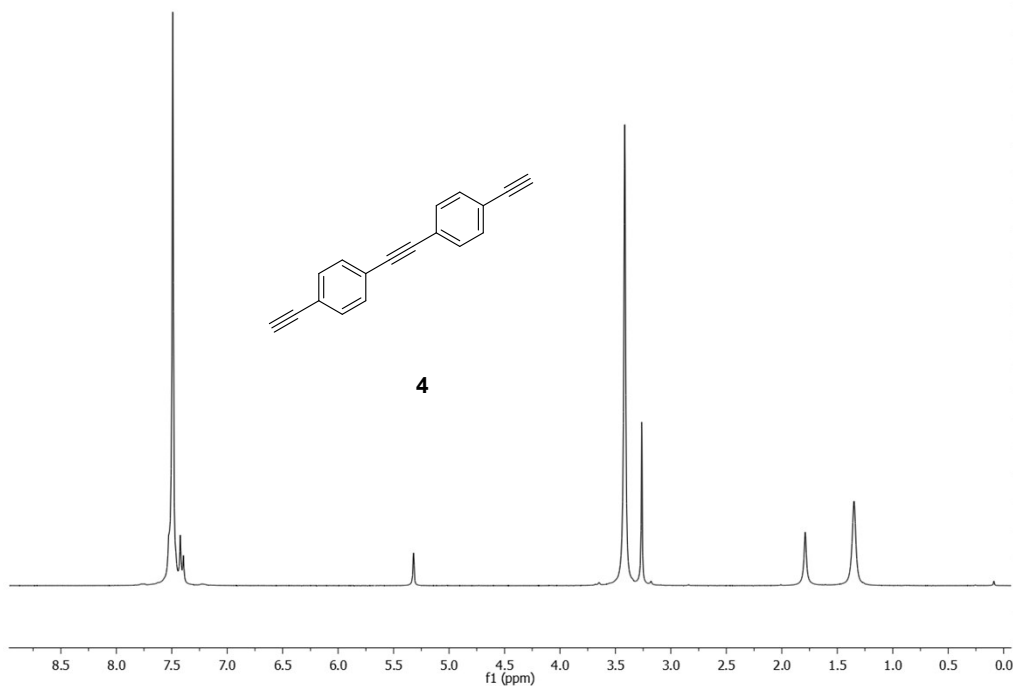


Fig. S17 ¹H-NMR spectra of 4,4'-Diethynyltolane (4) in CD₂Cl₂ The peak at 3.4 ppm is due to methanol.

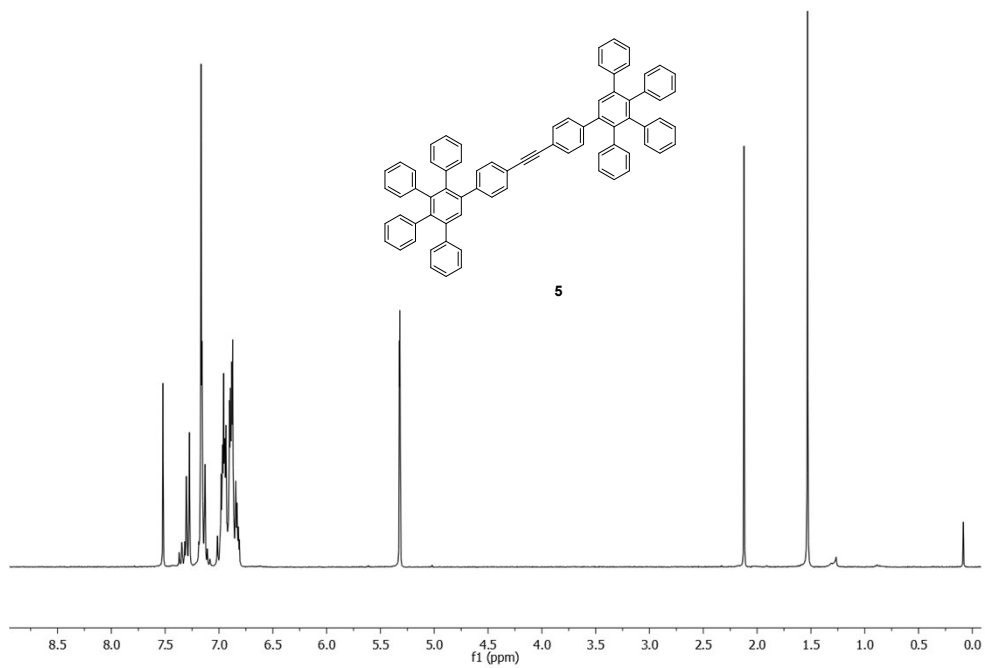


Fig. S18 ¹H-NMR spectra of 4,4'-(2,3,4,5-Tetraphenylbenzene)tolan (5) in CD₂Cl₂

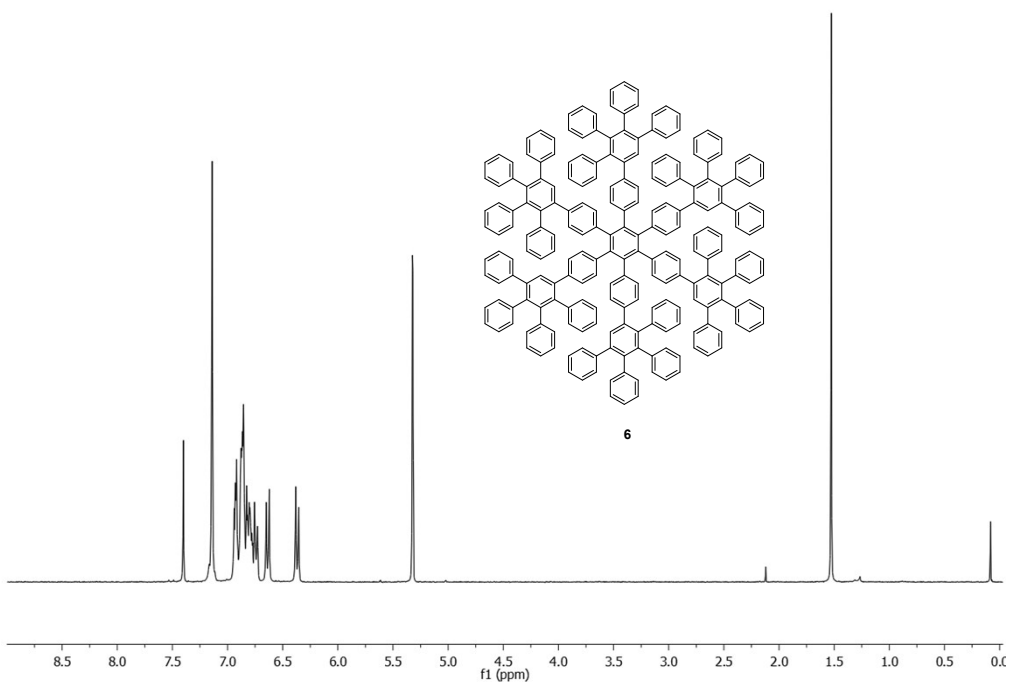


Fig. S19 ¹H-NMR spectra of 1,2,3,4,5,6-Hexakis(4',5',6'-triphenyl-1,1':2',1''-terphenyl)benzene (6) in CD₂Cl₂

7 References

- 1 L. Konnert, A. Gaudiard, F. Lamaty, J. Martinez and E. Colacino, *ACS Sustain. Chem. Eng.*, 2013, **1**, 1186–1191.
- 2 X. Feng, J. Wu, M. Ai, W. Pisula, L. Zhi, J. Rabe and K. Müllen, *Angew. Chemie Int. Ed.*, 2007, **46**, 3033–3036.
- 3 X. Feng, J. Wu, V. Enkelmann and K. Müllen, *Org. Lett.*, 2006, **8**, 1145–1148.
- 4 C. D. Simpson, J. D. Brand, A. J. Berresheim, L. Przybilla, H. J. Räder and K. Müllen, *Chem. - A Eur. J.*, 2002, **8**, 1424–1429.
- 5 S. Haferkamp, F. Fischer, W. Kraus and F. Emmerling, *Beilstein J. Org. Chem.*, 2017, **13**, 2010–2014.
- 6 L. Batzdorf, F. Fischer, M. Wilke, K.-J. Wenzel and F. Emmerling, *Angew. Chemie Int. Ed.*, 2015, **54**, 1799–1802.
- 7 P. A. Julien, I. Malvestiti and T. Friščić, *Beilstein J. Org. Chem.*, 2017, **13**, 2160–2168.
- 8 K. S. McKissic, J. T. Caruso, R. G. Blair and J. Mack, *Green Chem.*, 2014, **16**, 1628–1632.
- 9 F. Schneider, T. Szuppa, A. Stolle, B. Ondruschka and H. Hopf, *Green Chem.*, 2009, **11**, 1894–1899.
- 10 R. Schmidt, H. Martin Scholze and A. Stolle, *Int. J. Ind. Chem.*, 2016, **7**, 181–186.

8 Author contributions

Sven Grätz	Preparation of the manuscript; mechanochemical reactions and sample purification, GTM measurements, UV/VIS measurements
Doreen Beyer	Synthesis and characterization of the precursor compounds, C222 and C60; Major contribution to the ESI
Valeriya Tkachova	MALDI-TOF measurements
Sarah Hellmann	Mechanochemical reactions and sample purification, GTM measurements, ss-UV/Vis measurements
Reinhard Berger	Supervision of precursor synthesis and MALDI-TOF measurements, major contribution to the manuscript UV/VIS measurements
Xinliang Feng	Discussion of the results, supervision of precursor synthesis
Lars Borchardt	Project coordination and supervision